catalysts

MDPI

*Communication*

# Fabrication of Au Nanoparticle-Decorated $MoS_2$ Nanoslices as Efficient Electrocatalysts for Electrochemical Detection of Dopamine

**Huaiyin Chen [1], Huaijin Chen [2] and Ruoyu Hong [1,*]**

[1] College of Chemical Engineering, Fuzhou University, Fuzhou 350116, China
[2] State Grid Jining Power Supply Company, Jining 272000, China
* Correspondence: rhong@fzu.edu.cn; Tel.: +86-0591-22865220

Received: 10 July 2019; Accepted: 30 July 2019; Published: 30 July 2019


**Abstract:** Herein, $MoS_2$ nanoslices were simply prepared by using ultrasonic treatment, and were further decorated with Au nanoparticles (AuNPs) through an electrodeposition process to obtain the $MoS_2$/Au nanocomposites. The obtained nanocomposites display synergetic electrocatalytic effect for the oxidation of dopamine due to the large surface area and two-dimensional structure of the $MoS_2$ nanoslices, combining with the high catalytic activity and good conductivity of AuNPs. An electrochemical sensor was constructed based on $MoS_2$/Au-modified carbon paste electrode, for sensitive and quantitative determination of dopamine. The prepared electrochemical sensor proves excellent analytical performances: very high sensitivity, wide linear ranges (0.5–300 μM), and low detection limit (76 nM). Moreover, the dopamine sensor also displays high selectivity, good reproducibility and stability, and can be used in real sample analysis. The method of fabricating high-efficiency electrocatalysts and electrochemical sensors proposed in this study provides a good reference for developing more functionalized nanocomposites and for extending practical applications.

**Keywords:** dopamine; $MoS_2$; AuNPs; electrocatalyst; sensor

## 1. Introduction

Dopamine (DA) is a kind of key neurotransmitter, which plays an important role in the normal operation of multiple systems of human body [1–3]. Abnormal levels of DA in the body could cause several diseases, such as senile dementia, schizophrenia, and Alzheimer's disease [1,4]. Development of new materials, methods, or techniques to improve the accuracy and sensitivity in DA detection has great significance. Of the various methods of DA determination [2,5,6], the electrochemical sensor is preferred due to its fast response, high sensitivity, good selectivity, and low cost [7,8]. In order to get better response signals, various nanomaterials or nanocomposites have been used as electrocatalysts towards the oxidation of DA, such as carbon-based nanomaterials, noble metal nanoparticles [9], and conducting polymers [3,10–12]. Among these materials, two-dimensional (2D) nanomaterials or their corresponding composites play major roles. That is because 2D nanomaterials generally possess large conjugated layer structure and specific surface area, which can easily adsorb more aromatic and conjugated compounds on the basal plane via the van der Waals force [13,14]. Besides, there are many active sites on the edges and surface defects of 2D nanomaterials [15] that possess excellent catalytic activity towards many kinds of reactions including the electrochemical oxidation of DA. For example, Yang et al. [16] reported an electrochemical sensor for DA detection based on electrochemically reduced graphene oxide, which showed a low detection limit of 0.5 μM. Taylor et al. [17] demonstrated that poly(3,4-ethylene dioxythiophene)/graphene oxide as electrode modifying material could increase the sensitivity and meanwhile decrease the detection limit for the electrochemical detection of DA.

Besides graphene family, $MoS_2$ is another important 2D material that has been widely used in the fields of electronics, catalysis and sensing in recent years [18]. The 2D graphene-like structure, large surface area and available active sites also make $MoS_2$ suitable for the electrochemical catalysis and detection of DA. Pramoda et al. [19], among others, reported that $MoS_2$-reduced graphene oxide composite showed larger response signal than the sole reduced graphene oxide. In previous work [14], the poly(m-aminobenzenesulfonic acid)-reduced $MoS_2$ nanocomposites were used to construct electrochemical sensor for DA detection, which showed satisfactory analytical performance due to the synergetic catalytic effect of the nanocomposites. It is worth noting that Hun et al developed a photoelectrochemical sensor based on nano$MoS_2$, which showed nearly the widest linear detection range of 10 pM to 10 μM with a lowest detection limit of 2.3 pM [20], demonstrating the promising application prospects in the field of analytical chemistry.

Although numerous publications have been reported for the electrochemical detection of DA, the higher sensitivity and lower detection limit remain pending research topic. As a representative of noble metal nanoparticles, AuNPs were widely used in electrocatalysis and electrochemical sensing [21–24], including the sensing of DA [25–28]. However, the AuNPs are prone to aggregation, which will reduce their catalytic activity to a large extent. In situ fabrication of AuNPs on the supporting materials with large surface area or special structure has been nowadays available and favored.

In this study, AuNPs decorated $MoS_2$ nanoslices were prepared by sonicating bulk $MoS_2$ and further electrodeposition of AuNPs. The resultant $MoS_2$ nanoslices/AuNPs nanocomposites ($MoS_2$/Au) retained the 2D structure and large surface area of the $MoS_2$ nanoslices, which could support the deposition of AuNPs and prevent aggregation. As a result, the high catalytic activity of AuNPs was motivated, and the $MoS_2$/Au nanocomposites attained synergetic catalytic effect towards the electrochemical oxidation of DA, as shown in Scheme 1. An electrochemical sensor was constructed based on $MoS_2$/Au modified carbon paste electrode (CPE), for quantitative detection of DA. Under optimized condition, the sensor shows excellent analytical performance, superior than most of previously reported. The proposed method for fabricating efficient catalyst with synergetic catalysis and sensitive sensor provided a way for developing more functionalized nanocomposites and extending their applications.

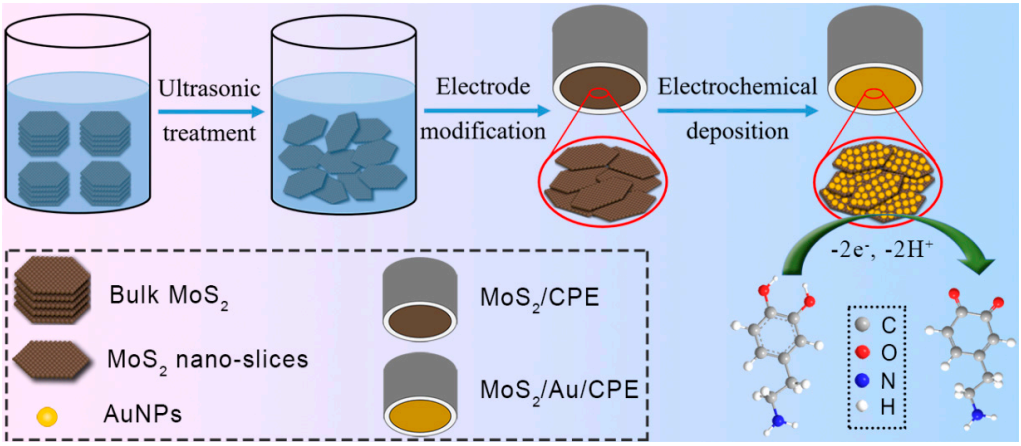


**Scheme 1.** Preparation of electrochemical sensor based on $MoS_2$/Au for Dopamine (DA) detection.

## 2. Results and Discussion

### *2.1. Characterization of Materials*

#### 2.1.1. Morphological Characterization

The morphologies of $MoS_2$ nanoslices and $MoS_2$/Au nanocomposites were characterized by scanning electron microscopy (SEM) and transmission electron microscopy (TEM). The results are

shown in Figure 1. From Figure 1A, it can be seen clearly that the obtained $MoS_2$ sample after ultrasonic treatment is thin slice-like shape. The nanoslices structure can also be confirmed from their TEM image (Figure 1C). This finding is consistent with our previous report, demonstrating that it is feasible to prepare $MoS_2$ nanoslices using ultrasonic treatment of bulk $MoS_2$ [7,14]. Compared with bulk $MoS_2$, the delaminated $MoS_2$ nanoslices should possess larger surface areas. Therefore, deposition of AuNPs on the surface of $MoS_2$ nanoslices could be more and uniform, as can be seen in the SEM image of $MoS_2$/Au (Figure 1B). The size of AuNPs on the surface of $MoS_2$ is ~10–20 nm, and no obvious aggregation of AuNPs is observed. Likewise, the dark and separate dots appearing on the TEM image of the nanocomposites (Figure 1D) confirm the successful fabrication of $MoS_2$/Au nanocomposites.

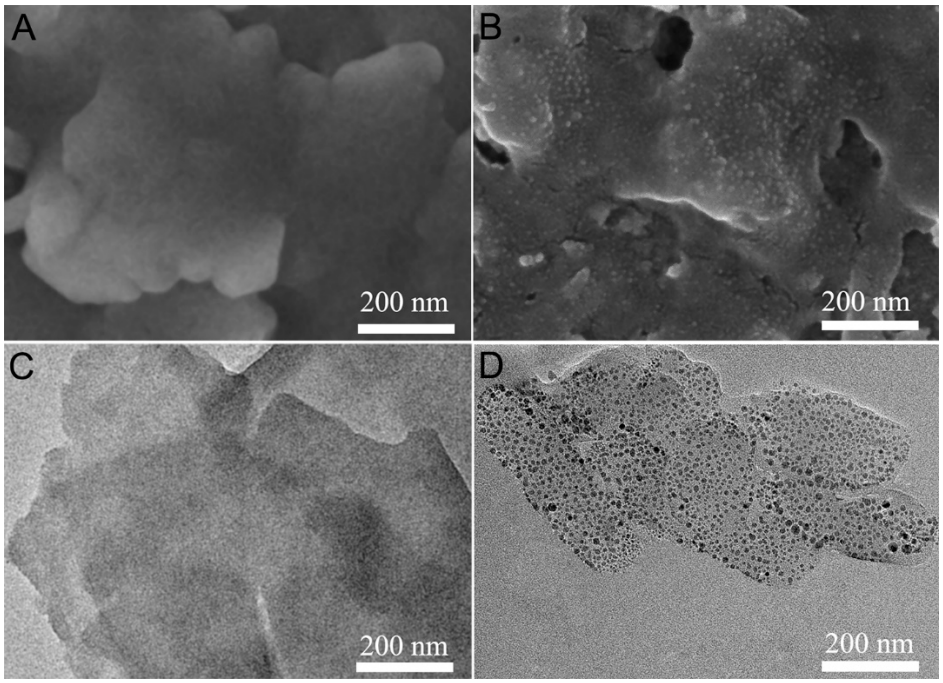


**Figure 1.** SEM images (**A**,**B**) and TEM images (**C**,**D**) of $MoS_2$ nanoslices (**A**,**C**) and $MoS_2$/Au nanocomposites (**B**,**D**).

### 2.1.2. Electrochemical characterization

In order to investigate the electrochemical properties of the prepared materials, cyclic voltammetry (CV) and electrochemical impedance electrochemical impedance spectra (EIS) measurements of bare CPE and various modified CPEs ($MoS_2$ nanoslice-modified CPE, AuNP-modified CPE, and $MoS_2$/Au-modified CPE were notated as $MoS_2$/CPE, Au/CPE, and $MoS_2$/Au/CPE, respectively) were carried out in 1.0 mM $[Fe(CN)_6]^{3-/4-}$ indicator solution (pH 7.0). As displayed in Figure 2A, no apparent redox peaks are observed on the CV curve of bare CPE, indicating the poor conductivity and very small electroactive surface area, similarly to those reported by Yang et al. [29]. A couple of redox peaks appear on the CV curves of $MoS_2$/CPE, Au/CPE, and $MoS_2$/Au/CPE, and the peak current values increase in turn, indicating the positive effects of the prepared nanomaterials on the improvement of the conductivity and electroactive surface area of CPE. However, compared with $MoS_2$/CPE and Au/CPE, $MoS_2$/Au/CPE shows the largest peak current values, implying the higher conductivity and electroactive surface area of $MoS_2$/Au nanocomposites than the single nanomaterials. This is because the combination of $MoS_2$ nanoslices and AuNPs can not only retain the large surface area of $MoS_2$, but also effectively avoid the aggregation of AuNPs in deposition process. The EIS test results are illustrated in Figure 2B, from the Nyquist plot it is found that the semicircular capacitive loop of CPE, $MoS_2$/CPE, Au/CPE, and $MoS_2$/Au/CPE decreases in sequence, indicating the gradually decreasing charge-transfer

resistance ($R_{ct}$), that is, $MoS_2$/Au/CPE facilitate the charge transfer in a greater degree [2,30]. It is in line with and further confirms the result drawn from CV tests.

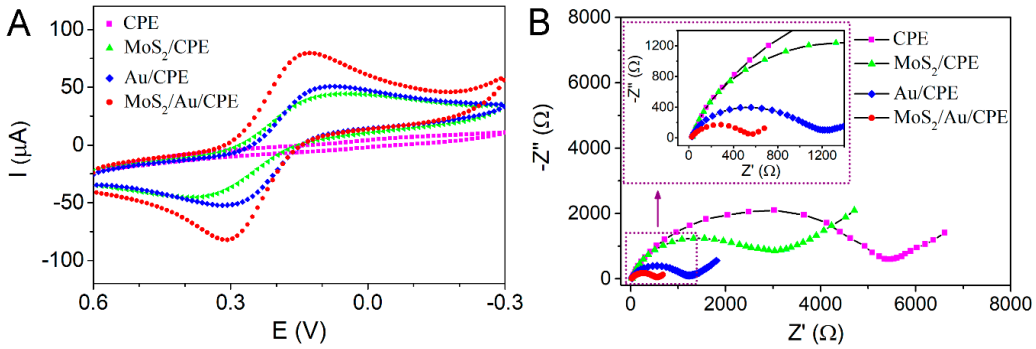


**Figure 2.** The (**A**) CV and (**B**) EIS curves recorded at bare CPE, $MoS_2$/CPE, Au/CPE and $MoS_2$/Au/CPE in 1.0 mM $[Fe(CN)_6]^{3-/4-}$ solution (pH 7.0).

## 2.2. The Elextrochemical Behaviors of DA

The catalytic effects of the prepared nanomaterials towards the electrochemical oxidations of DA were investigated by CV measurements. Figure 3A shows the different electrocatalytic effects of the various nanomaterials. It can be seen that a couple of small and irreversible redox peaks present at the CV curve of CPE, and the difference between anodic peak potential ($E_{pa}$) and cathodic peak potential ($E_{pc}$) exceeds 0.5 V, and $E_{pa}$ value is greater than 0.4 V, which indicates the inferior catalytic effect of bare CPE towards the oxidation of DA. Compared with bare CPE, $MoS_2$/CPE and Au/CPE show more apparent redox peaks and smaller peak potential differences, demonstrating both $MoS_2$ nanoslices and AuNPs have electrocatalytic effect on the oxidation of DA. The large surface area and 2D conjugated structure of $MoS_2$ nanoslices could physically adsorb more aromatic and conjugated compounds on the basal plane via the van der Waals force [13,14]. The AuNPs has an intrinsic catalytic property and excellent conductivity. However, the $MoS_2$/Au/CPE displays larger redox peaks and smaller peak potential difference than the sole nanomaterials modified CPE, indicating the $MoS_2$/Au nanocomposites get the synergistic catalytic activity towards the oxidation of DA. It is attributed to the large electroactive surface area, special structure that can adsorb DA molecules and the high conductivity, as well as the retain of the catalytic activity of AuNPs.

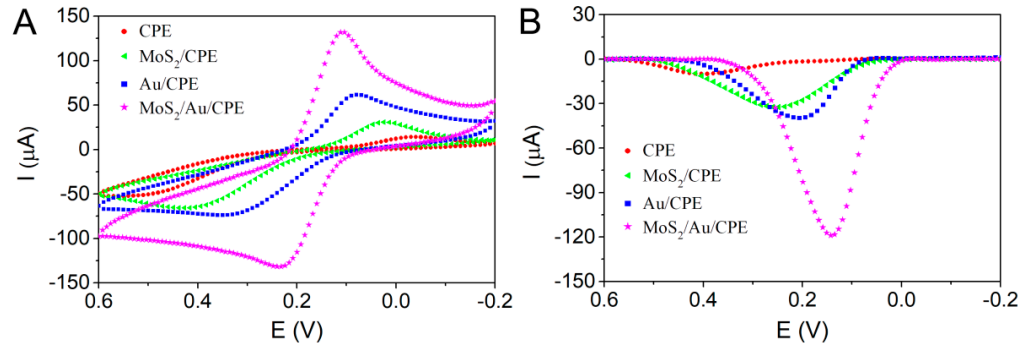


**Figure 3.** The cyclic voltammetry (CV) (**A**) and differential pulse voltammetry (DPV) (**B**) curves recorded at bare CPE, $MoS_2$/CPE, Au/CPE, and $MoS_2$/Au/CPE in 0.1M PBS solution (pH 7.0) containing 1.0 mM DA.

In order to investigate the electrochemical catalytic effects of analytical performance of different electrodes more clearly and readily, differential pulse voltammetry (DPV) technique was adopted to measure the oxidation process of DA. As observed from Figure 3B, the DPV curves show the same variation trend with that in the oxidation process of CV curves, that is, the $E_{pa}$ values of bare CPE,

$MoS_2$/CPE, Au/CPE, and $MoS_2$/Au/CPE decrease in turn while the anodic peak current ($I_{pa}$) values increase. The result that $MoS_2$/Au/CPE possesses the best electrocatalytic effect towards the oxidation of DA coincides with that obtained from CV measurements. Therefore, the electrochemical sensor based on $MoS_2$/Au nanocomposites for the detection of DA was constructed and considered feasible.

To further study the electrochemical behavior of DA at $MoS_2$/Au/CPE, CV measurements of 0.2 mM DA at different scan rate (υ) were performed, and the results are shown in Figure S1. It is observed from Figure S1A that both the $I_{pa}$ values and the cathodic peak current ($I_{pc}$) values increase with the scan rate gradually increasing from 20 to 300 mV/s. Figure S1B shows the linear relationships between redox peak currents and scan rates, which can be denoted by Equations (1) and (2), respectively.

$$I_{pa}\ (\mu A) = -0.1523\upsilon - 6.0034\ (R^2 = 0.9941) \quad (1)$$

$$I_{pc}\ (\mu A) = 0.1683\upsilon + 4.7878\ (R^2 = 0.9977) \quad (2)$$

The results confirm that DA molecules can be adsorbed onto the surface of the $MoS_2$/Au/CPE, and indicate the electrode reaction of DA is an adsorption-controlled process [14,31,32].

### *2.3. Condition Optimization for Electrochemical Detection of DA*

For the purpose of obtaining the optimal response signals for DA detection, the condition optimization was conducted. For the electrochemical deposition of AuNPs on $MoS_2$/CPE, the deposition time has an important effect on the amount of AuNPs, and then results in different response signals for DA detection. As exhibited in Figure S2, with the deposition time increasing from 100 to 500 s, the $I_{pa}$ value increases at first and reaches the maximum at 300 s, and then decreases with further increase of the deposition time. With the increase of deposition time from 100 to 300 s, more AuNPs were produced. The conductivity, surface area, and catalytic activity of the $MoS_2$/Au/CPE were improved correspondingly. However, too long deposition time caused the stack and aggregation of abundant AuNPs, reducing the active surface area and hence resulting in the decreased $I_{pa}$ values. Therefore, 300 s was the optimal deposition time of AuNPs in this experiment.

The electrochemical oxidation of DA is a kind of proton-involved reaction. The pH of detection solution has an effect on the electrocatalytic behavior of DA. This effect was studied by DPV measurements and the results are displayed in Figure S3A. It is observed that the pH has important effects on both $E_{pa}$ and $I_{pa}$, and the effects are more clearly depicted in Figure S3B. With the increase of pH from 5.0 to 9.0, the $E_{pa}$ value of DA decreases gradually, and it has a linear relationship with the pH, expressed by

$$E_{pa}\ (V) = -0.0536pH + 0.522\ (R^2 = 0.9981). \quad (3)$$

The slope of the linear equation ($E_{pa}$/pH) was -53.6 mV/pH that is close to the theoretical value for an equal number of proton and electron involved reaction (−59 mV/pH at 25 °C), implying the oxidation of DA at $MoS_2$/Au/CPE is a 2-electron and 2-proton involved process [10,25,33]. Furthermore, it shows that the $I_{pa}$ value of DA increases with increasing pH value from 5.0 to 7.0, and then decreases with the further increase of pH value from 7.0 to 9.0. Therefore, pH 7.0 is the optimal for DA detection.

### *2.4. Electrochemical Detection of DA*

For analytical detection, the sensitivity and accuracy are the key. DPV measurement was performed for the quantitative detection of DA under the optimal conditions. Figure 4A shows the DPV curves of DA with a variety of different concentrations (from 0.5 to 300 μM) recorded at $MoS_2$/Au/CPE. It is clearly observed that the current responses enlarge with the increase of the concentration, and even in very low concentration the anodic peaks are still apparently found from the inserted plot. Figure 4B

displays a linear relationship of the $I_{pa}$ values versus the concentrations of DA ranging from 0.5 to 300 μM. The linear regression equation is expressed by

$$|I_{pa}| (\mu A) = 0.110C (\mu M) + 1.786 (R^2 = 0.9977), \quad (4)$$

where $|I_{pa}|$ denotes the $I_{pa}$ value in this paper. The detection sensitivity (the slope of linear equation) is up to 0.11 A/M, which is much higher than that in previous reports [10,34,35]. The detection limit was estimated to be 76 nM, based on the result analysis above and the formula

$$D = 3S_b/m, \quad (5)$$

where $S_b$ denotes the standard deviation of blank signals of 10 parallel measurements and $m$ is the detection sensitivity [14,25]. The comparison of the analytical performances of $MoS_2$/Au/CPE with that of other reported electrochemical sensors is shown in Table 1. It can be found this study provides a relatively low detection limit and a wide linear range for DA detection.

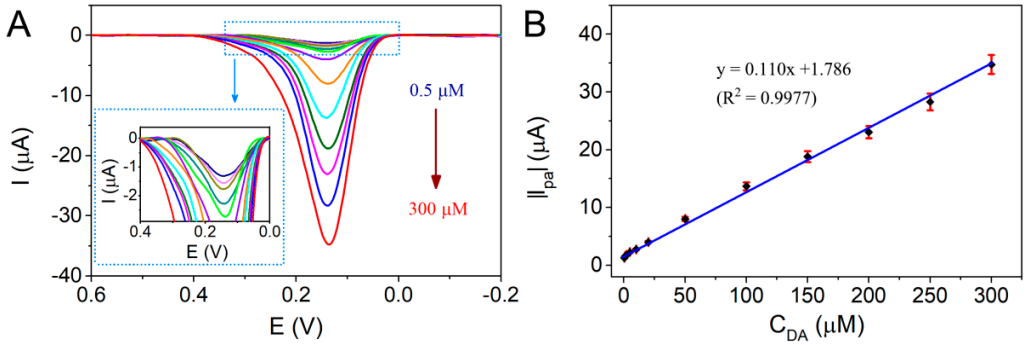


**Figure 4.** (**A**) The DPV curves of $MoS_2$/Au/CPE in 0.1M PBS solution (pH 7.0) containing DA with a series of concentrations (0.5, 1, 2, 5, 10, 20, 50, 100, 150, 200, 250, and 300 μM) and (**B**) the relationship of $I_{pa}$ value versus the concentration of DA.

**Table 1.** Comparison of electroanalytical performances of different modified electrodes for DA detection.

| Electrode | Detection Method | Linear Range (μM) | Detection Limit (μM) | Reference |
|---|---|---|---|---|
| 3D-$MoS_2$/rGO [1]/Au@GCE | DPV | 0.3–198.3 | 0.11 | [3] |
| $MoS_2$/PEDOT [2]/GCE | DPV | 1–80 | 0.52 | [12] |
| PABSA-r$MoS_2$ [3]/CPE | DPV | 1–50 | 0.22 | [14] |
| GO [4]/GCE | DPV | 1–15 | 0.27 | [36] |
| porous AuNSs [5]/GCE | DPV | 2–298 | 0.28 | [37] |
| Pd/rGO [1]/GCE | DPV | 0.45–421 | 0.18 | [38] |
| $MoS_2$/Au/CPE | DPV | 0.5–300 | 0.076 | This work |

[1] rGO: reduced graphene oxide; [2] PEDOT: poly(3,4-ethylenedioxythiophene); [3] PABSA-r$MoS_2$: poly(m-aminobenzenesulfonic acid)-reduced $MoS_2$; [4] GO: graphene oxide; [5] AuNSs: Au nanosheets.

### *2.5. Selectivity of the Eectrochemical Sensor*

Interference tests from common foreign substances were carried out to evaluate the anti-interference performance of the proposed electrochemical DA sensor. As listed in Table S1, 10 mM $KNO_3$, NaCl, $CaCl_2$, and $MgSO_4$ or 2 mM glucose and citric acid has little influence on the current response of 50 μM DA (the relative error is within ±5%).

Ascorbic acid (AA) and uric acid (UA) are the main interferents that always interfere the electrochemical detection of DA. The anti-interference towards AA and UA is a key performance of an electrochemical DA sensor. Figure S4 shows the DPV responses of the proposed electrochemical sensor for 50 μM DA with AA and UA in different concentrations, it can be seen that the anodic peaks

are separate, and the presence of 500 μM AA and 100 μM UA have no obvious influence on the $I_{pa}$ value of 50 μM DA, demonstrating the high selectivity of the electrochemical DA sensor.

### 2.6. Reproducibility and Stability of the Electrochemical Sensor

The reproducibility of the proposed electrochemical sensor was evaluated through the parallel measurements of DPV responses of 10 μM DA at five independent $MoS_2$/Au/CPEs. The results are shown in Figure S5A. The relative standard deviation (RSD) of these $I_{pa}$ values was calculated as 4.09%, indicating a good reproducibility. Besides, the stability of the prepared sensor was also investigated by the measurement of the DPV response of 10 μM DA after storage at 4 °C for a period of time. Figure S5B exhibits that the $I_{pa}$ value retains about 96.4% of its original value after 5 days and ~90.3% after 20 days, demonstrating an acceptable long-time stability.

### 2.7. Real Sample Analysis

Urine samples were tested using standard addition method to evaluate the analytical performance of the DA sensor in real sample detections. Table 2 shows the detection results, from which it is found that the recoveries range from 96.3% to 104%, implying that the proposed electrochemical sensor has a satisfactory performance for DA detection in the real samples.

**Table 2.** Detection of DA in urine samples (n = 3).

| Sample No. | DA Added (μM) | DA Found (μM) | Recovery (%) | RSD (%) |
|---|---|---|---|---|
| 1 | 0 | Not found | – | – |
| 2 | 10 | 9.63 ± 0.42 | 96.3 ± 4.2 | 4.2 |
| 3 | 20 | 20.8 ± 0.62 | 104 ± 3.1 | 3.5 |
| 4 | 40 | 38.9 ± 1.45 | 97.3 ± 3.6 | 3.8 |

## 3. Materials and Methods

### 3.1. Reagents and Apparatus

#### 3.1.1. Reagents

Bulk $MoS_2$ (powder, <2 μm, 98%) and dopamine hydrochloride were obtained from Sigma-Aldrich (St. Louis, MO, USA). Ascorbic acid (99.99%) and uric acid (99%) were bought from Aladdin (Shanghai, China). $HAuCl_4 \cdot 4H_2O$ (99.9%), $K_3Fe(CN)_6$ (≥99.0%) and $K_4Fe(CN)_6 \cdot 3H_2O$ (≥99.5%) were purchased from Sinopharm Chemical Reagent Co., Ltd. (Shanghai, China). N,N-dimethylformamide (DMF, 99%), $NaH_2PO_4 \cdot 2H_2O$ (≥99%) and $Na_2HPO_4 \cdot 2H_2O$ (≥99%) were obtained from Adamas-beta (Shanghai, China). Other regents used in this study were provided by domestic regular reagent companies, and directly used without any treatment. Deionized water from a Milli-Q ultrapure water purification system was used for the preparation of aqueous solution. Phosphate buffer solution ((PBS) 0.1 M) consisting of $NaH_2PO_4/Na_2HPO_4$ was used as supporting electrolyte, and its pH was adjusted by 0.1 M HCl or NaOH aqueous solution. 1.0 mM $[Fe(CN)_6]^{3-/4-}$ aqueous solution (pH 7.0) containing 0.1 M KCl that prepared with $K_3Fe(CN)_6$, $K_4Fe(CN)_6 \cdot 3H_2O$ and KCl was used as electroactive indicator solution.

#### 3.1.2. Apparatus

The electrochemical tests were conducted on a CHI 760D electrochemical workstation (Shanghai CH Instrument Company, Shanghai, China) with a three-electrode system, in which a bare CPE or modified CPE acted as working electrode and a saturated calomel electrode and a platinum wire acted as reference electrode and counter electrode, respectively. The ultrasonic treatment was carried out using a KQ-500B ultrasonic cleaner (Kunshan Ultrasonic Instruments Co., Ltd., Kunshan, China). The measurements of pH values were performed with a PHS-25 digital pH meter (Shanghai Leici

Factory, Shanghai, China). A JSM-6700F SEM (JEOL, Tokyo, Japan) and JEM-2100 TEM (JEOL, Tokyo, Japan) were used for the morphological characterizations.

### *3.2. Fbrication of Modified Electrodes*

CPE was fabricated by the method reported previously [39]. Briefly, graphite powder and paraffin with the mass ratio of 3:1 were homogeneously mixed by stirring at 60 °C, and then the homogeneous carbon paste was filled in a glass tube (Φ = 4 mm) and compacted after vibration. A copper wire was inserted in the carbon paste as a conductive wire. It is required to be polished on a paper before use.

$MoS_2$ nanoslice dispersion was prepared by ultrasonic treatment of bulk $MoS_2$ in DMF for 4 h with the $MoS_2$ concentration of 1 mg/mL [14]. 20 μL of the dispersion was dripped on the tip of CPE, then $MoS_2$/CPE was obtained after the dispersion naturally dried in the air.

$MoS_2$/Au/CPE was prepared through potentiostatic electrodeposition of AuNPs at $MoS_2$/CPE in 0.1 M PBS containing 2.0 mM $HAuCl_4$ under −0.2 V for a certain time. It should be noted that the $MoS_2$/Au/CPE used in this study was prepared under the deposition time of 300 s except in the experiment of condition optimization.

As a contrast, Au/CPE was also fabricated under the same condition at CPE instead of $MoS_2$/CPE.

### *3.3. Electrochemical Measurements*

For CV measurements in 1.0 mM $[Fe(CN)_6]^{3-/4-}$ indicator solution (pH 7.0), the potential was scanned between 0.6 and −0.3 V with a scan rate of 0.1 V/s, while in 0.1 M PBS (pH 7.0) containing 1.0 mM DA, the potential range was scanned between 0.6 and −0.2 V with the same scan rate. The potential and the frequency range for EIS measurements in 1.0 mM $[Fe(CN)_6]^{3-/4-}$ indicator solution (pH 7.0) were set as 0.17 V and 10 kHz–0.1 Hz. For DPV measurements, the potential range, scan rate, pulse width, pulse amplitude, and pulse period were set as from −0.2 to 0.6 V, 0.05 V $s^{-1}$, 0.2 s, 0.05 V, and 0.5 s, respectively.

Unless otherwise stated, all the experiment results in this study were the average of three parallel measurements.

## 4. Conclusions

$MoS_2$ nanoslices and AuNPs nanocomposites were prepared by using ultrasonic treatment and electrodeposition technique. The obtained $MoS_2$/Au nanocomposites retained the large surface area and 2D slice-like structure of $MoS_2$ nanoslices and, simultaneously, the high catalytic activity and good conductivity of AuNPs, resulting in synergetic electrocatalytic effect for the oxidation of DA. The electrochemical sensor constructed based on $MoS_2$/Au nanocomposites shows excellent analytical performances for the DA detection, including very high sensitivity (0.11 A/M), wide linear range (0.5–300 μM), low detection limit (76 nM), high selectivity, and good reproducibility, stability, and availability in real sample analysis.

**Supplementary Materials:** The following are available online at http://www.mdpi.com/2073-4344/9/8/653/s1. Figure S1: (A) The CV curves of $MoS_2$/Au/CPE in 0.1M PBS (pH 7.0) containing 0.2 mM DA at a series of scan rate (from a to g: 20, 30, 50, 80, 100, 150, 200, 300 mV/s), (B) the linear relationships of $I_{pa}$ and $I_{pc}$ versus the scan rate; Figure S2: (A) the DPV curves of $MoS_2$/Au/CPE prepared under different electrodeposition time of AuNPs in 0.1M PBS (pH 7.0) containing 1.0 mM DA, (B) the corresponding variation of $I_{pa}$ value with the increase of the electrodeposition time; Figure S3: (A) the DPV curves of $MoS_2$/Au/CPE in 0.1M PBS (pH 7.0) containing 1.0 mM DA at different pH, (B) the corresponding variation of $I_{pa}$ and $E_{pa}$ values with the change of pH; Table S1: Detection of 50 μM DA in the presence of the common substance; Figure S4: The DPV curves of $MoS_2$/Au/CPE in 0.1M PBS (pH 7.0) containing 50 μM DA and (a) 0μM AA + 0μM UA, (b) 100 μM AA + 20 μM UA, (c) 300 μM AA + 60 μM UA, and (d) 500 μM AA + 100 μM UA; Figure S5: (A) the $I_{pa}$ values of DPV measurements recorded in 0.1M PBS (pH 7.0) containing 10 μM DA at five independent $MoS_2$/Au/CPEs, (B) the $I_{pa}$ values of DPV measurements in 0.1M PBS (pH 7.0) containing 10 μM DA at $MoS_2$/Au/CPE after storage for different periods of time.

**Author Contributions:** Conceptualization, H.C. (Huaiyin Chen) and R.H.; methodology, H.C. (Huaiyin Chen); software, H.C. (Huaiyin Chen) and H.C. (Huaijin Chen); validation, H.C. (Huaiyin Chen), H.C. (Huaijin Chen), and R.H.; formal analysis, H.C. (Huaiyin Chen); investigation, H.C. (Huaiyin Chen) and H.C. (Huaijin Chen);

resources, R.H.; data curation, H.C. (Huaiyin Chen); writing—original draft preparation, H.C. (Huaiyin Chen); writing—review and editing, H.C. (Huaiyin Chen), H.C. (Huaijin Chen), and R.H.; visualization, H.C. (Huaiyin Chen); supervision, R.H.; project administration, R.H.; funding acquisition, R.H.

**Funding:** This research was funded by the National Natural Science Foundation of China (No. 21675092), Minjiang Scholarship of Fujian Province (No. Min-Gaojiao[2010]-117), Central Government-Guided Fund for Local Economic Development (No. 830170778), R&D Fund for Strategic Emerging Industry of Fujian Province (No. 82918001), and Teaching and Researching Fund for Young Staff of Fujian Educational Department (No. JT180040).

**Conflicts of Interest:** The authors declare no conflict of interest. The funders had no role in the design of the study; in the collection, analyses, or interpretation of data; in the writing of the manuscript, or in the decision to publish the results.

## References

1. Oh, J.W.; Yoon, Y.W.; Heo, J.; Yu, J.; Kim, H.; Kim, T.H. Electrochemical detection of nanomolar dopamine in the presence of neurophysiological concentration of ascorbic acid and uric acid using charge-coated carbon nanotubes via facile and green preparation. *Talanta* **2016**, *147*, 453–459. [CrossRef] [PubMed]
2. Rezaei, B.; Boroujeni, M.K.; Ensafi, A.A. Fabrication of DNA, o-phenylenediamine, and gold nanoparticle bioimprinted polymer electrochemical sensor for the determination of dopamine. *Biosens. Bioelectron.* **2015**, *66*, 490–496. [CrossRef] [PubMed]
3. Zhao, Y.; Zhou, J.; Jia, Z.; Huo, D.; Liu, Q.; Zhong, D.; Hu, Y.; Yang, M.; Bian, M.; Hou, C. In-situ growth of gold nanoparticles on a 3D-network consisting of a $MoS_2$/rGO nanocomposite for simultaneous voltammetric determination of ascorbic acid, dopamine and uric acid. *Mikrochim. Acta* **2019**, *186*, 92. [CrossRef] [PubMed]
4. Gu, X.; Jiang, G.; Jiang, G.; Chen, T.; Zhan, W.; Li, X.; Wu, S.; Tian, S. Detection of dopamine on a mercapto-terminated hexanuclear Fe(III) cluster modified gold electrode. *Talanta* **2015**, *137*, 189–196. [CrossRef] [PubMed]
5. Pruneanu, S.; Biris, A.R.; Pogacean, F.; Socaci, C.; Coros, M.; Rosu, M.C.; Watanabe, F.; Biris, A.S. The influence of uric and ascorbic acid on the electrochemical detection of dopamine using graphene-modified electrodes. *Electrochim. Acta* **2015**, *154*, 197–204. [CrossRef]
6. Canevari, T.C.; Nakamura, M.; Cincotto, F.H.; de Melo, F.M.; Toma, H.E. High performance electrochemical sensors for dopamine and epinephrine using nanocrystalline carbon quantum dots obtained under controlled chronoamperometric conditions. *Electrochim. Acta* **2016**, *209*, 464–470. [CrossRef]
7. Yang, T.; Chen, H.; Ge, T.; Wang, J.; Li, W.; Jiao, K. Highly sensitive determination of chloramphenicol based on thin-layered $MoS_2$/polyaniline nanocomposite. *Talanta* **2015**, *144*, 1324–1328. [CrossRef]
8. Bergman, J.; Mellander, L.; Wang, Y.; Cans, A.-S. Co-detection of dopamine and glucose with high temporal resolution. *Catalysts* **2018**, *8*, 34. [CrossRef]
9. Mazloum-Ardakani, M.; Abolhasani, M.; Mirjalili, B.F.; Sheikh-Mohseni, M.A.; Dehghani-Firouzabadi, A.; Khoshroo, A. Electrocatalysis of dopamine in the presence of uric acid and folic acid on modified carbon nanotube paste electrode. *Chin. J. Catal.* **2014**, *35*, 201–209. [CrossRef]
10. Huang, K.-J.; Zhang, J.-Z.; Liu, Y.-J.; Wang, L.-L. Novel electrochemical sensing platform based on molybdenum disulfide nanosheets-polyaniline composites and Au nanoparticles. *Sens. Actuators B* **2014**, *194*, 303–310. [CrossRef]
11. Qi, S.; Zhao, B.; Tang, H.; Jiang, X. Determination of ascorbic acid, dopamine, and uric acid by a novel electrochemical sensor based on pristine graphene. *Electrochim. Acta* **2015**, *161*, 395–402. [CrossRef]
12. Li, Y.; Lin, H.; Peng, H.; Qi, R.; Luo, C. A glassy carbon electrode modified with $MoS_2$ nanosheets and poly(3,4-ethylenedioxythiophene) for simultaneous electrochemical detection of ascorbic acid, dopamine and uric acid. *Microchim. Acta* **2016**, *183*, 2517–2523. [CrossRef]
13. Zhu, C.; Zeng, Z.; Li, H.; Li, F.; Fan, C.; Zhang, H. Single-layer $MoS_2$-based nanoprobes for homogeneous detection of biomolecules. *J. Am. Chem. Soc.* **2013**, *135*, 5998–6001. [CrossRef] [PubMed]
14. Yang, T.; Chen, H.; Jing, C.; Luo, S.; Li, W.; Jiao, K. Using poly(m-aminobenzenesulfonic acid)-reduced $MoS_2$ nanocomposite synergistic electrocatalysis for determination of dopamine. *Sens. Actuators B* **2017**, *249*, 451–457. [CrossRef]
15. Chia, X.; Pumera, M. Characteristics and performance of two-dimensional materials for electrocatalysis. *Nat. Catal.* **2018**, *1*, 909–921. [CrossRef]

16. Yang, L.; Liu, D.; Huang, J.; You, T. Simultaneous determination of dopamine, ascorbic acid and uric acid at electrochemically reduced graphene oxide modified electrode. *Sens. Actuators B* **2014**, *193*, 166–172. [CrossRef]
17. Taylor, I.M.; Robbins, E.M.; Catt, K.A.; Cody, P.A.; Happe, C.L.; Cui, X.T. Enhanced dopamine detection sensitivity by PEDOT/graphene oxide coating on in vivo carbon fiber electrodes. *Biosens. Bioelectron.* **2017**, *89*, 400–410. [CrossRef] [PubMed]
18. Chen, H.-Y.; Wang, J.; Meng, L.; Yang, T.; Jiao, K. Thin-layered $MoS_2$/polyaniline nanocomposite for highly sensitive electrochemical detection of chloramphenicol. *Chin. Chem. Lett.* **2016**, *27*, 231–234. [CrossRef]
19. Pramoda, K.; Moses, K.; Maitra, U.; Rao, C.N.R. Superior performance of a $MoS_2$-RGO composite and a borocarbonitride in the electrochemical detection of dopamine, uric acid and adenine. *Electroanalysis* **2015**, *27*, 1892–1898. [CrossRef]
20. Hun, X.; Wang, S.; Wang, S.; Zhao, J.; Luo, X. A photoelectrochemical sensor for ultrasensitive dopamine detection based on single-layer Nano$MoS_2$ modified gold electrode. *Sens. Actuators B* **2017**, *249*, 83–89. [CrossRef]
21. Yadav, D.K.; Ganesan, V.; Sonkar, P.K.; Gupta, R.; Rastogi, P.K. Electrochemical investigation of gold nanoparticles incorporated zinc based metal-organic framework for selective recognition of nitrite and nitrobenzene. *Electrochim. Acta* **2016**, *200*, 276–282. [CrossRef]
22. Lin, P.; Chai, F.; Zhang, R.; Xu, G.; Fan, X.; Luo, X. Electrochemical synthesis of poly(3,4-ethylenedioxythiophene) doped with gold nanoparticles, and its application to nitrite sensing. *Microchim. Acta* **2016**, *183*, 1235–1241. [CrossRef]
23. Chen, H.; Yang, T.; Liu, F.; Li, W. Electrodeposition of gold nanoparticles on Cu-based metal-organic framework for the electrochemical detection of nitrite. *Sens. Actuators B* **2019**, *286*, 401–407. [CrossRef]
24. Wang, Y.; Wang, L.; Chen, H.; Hu, X.; Ma, S. Fabrication of highly sensitive and stable hydroxylamine electrochemical sensor based on gold nanoparticles and metal-metalloporphyrin framework modified electrode. *ACS Appl. Mater. Interfaces* **2016**, *8*, 18173–18181. [CrossRef] [PubMed]
25. Rezaei, B.; Havakeshian, E.; Ensafi, A.A. Decoration of nanoporous stainless steel with nanostructured gold via galvanic replacement reaction and its application for electrochemical determination of dopamine. *Sens. Actuators B* **2015**, *213*, 484–492. [CrossRef]
26. Khan, M.Z.H.; Liu, X.Q.; Tang, Y.F.; Zhu, J.H.; Hu, W.P.; Liu, X.H. A glassy carbon electrode modified with a composite consisting of gold nanoparticle, reduced graphene oxide and poly(L-arginine) for simultaneous voltammetric determination of dopamine, serotonin and L-tryptophan. *Microchim. Acta* **2018**, *185*, 439. [CrossRef] [PubMed]
27. Li, C.; Chen, X.J.; Zhang, Z.; Tang, J.L.; Zhang, B.L. Gold nanoparticle-DNA conjugates enhanced determination of dopamine by aptamer-based microcantilever array sensor. *Sens. Actuators B* **2018**, *275*, 25–30. [CrossRef]
28. Mei, X.R.; Wei, Q.P.; Long, H.Y.; Yu, Z.M.; Deng, Z.J.; Meng, L.C.; Wang, J.; Luo, J.T.; Lin, C.T.; Ma, L.; et al. Long-term stability of Au nanoparticle-anchored porous boron-doped diamond hybrid electrode for enhanced dopamine detection. *Electrochim. Acta* **2018**, *271*, 84–91. [CrossRef]
29. Yang, T.; Chen, H.; Qiu, Z.; Yu, R.; Luo, S.; Li, W.; Jiao, K. Direct vibrio DNA sensing adopting highly stable graphene-flavin mononucleotide aqueous dispersion modified interface. *ACS Appl. Mater. Interfaces* **2018**, *10*, 4540–4547. [CrossRef]
30. Hu, L.; Ren, Y.; Yang, H.; Xu, Q. Fabrication of 3D hierarchical $MoS_2$/polyaniline and $MoS_2$/C architectures for lithium-ion battery applications. *ACS Appl. Mater. Interfaces* **2014**, *6*, 14644–14652. [CrossRef]
31. Yao, Y.; Wen, Y.; Xu, J.; Zhang, L.; Duan, X. Application of commercial poly(3,4-ethylenedioxy-thiophene): poly(styrene sulfonate) for electrochemical sensing of dopamine. *J. Serb. Chem. Soc.* **2013**, *78*, 1397–1411. [CrossRef]
32. Wang, P.; Li, Y.; Huang, X.; Wang, L. Fabrication of layer-by-layer modified multilayer films containing choline and gold nanoparticles and its sensing application for electrochemical determination of dopamine and uric acid. *Talanta* **2007**, *73*, 431–437. [CrossRef] [PubMed]
33. Zhang, M.; Gong, K.; Zhang, H.; Mao, L. Layer-by-layer assembled carbon nanotubes for selective determination of dopamine in the presence of ascorbic acid. *Biosens. Bioelectron.* **2005**, *20*, 1270–1276. [CrossRef] [PubMed]

34. Hammami, A.; Sahli, R.; Raouafi, N. Indirect amperometric sensing of dopamine using a redox-switchable naphthoquinone-terminated self-assembled monolayer on gold electrode. *Microchim. Acta* **2016**, *183*, 1137–1144. [CrossRef]
35. Ma, L.; Zhang, Q.; Wu, C.; Zhang, Y.; Zeng, L. PtNi bimetallic nanoparticles loaded $MoS_2$ nanosheets: Preparation and electrochemical sensing application for the detection of dopamine and uric acid. *Anal. Chim. Acta* **2019**, *1055*, 17–25. [CrossRef] [PubMed]
36. Fritzen-Garcia, M.B.; Monteiro, F.F.; Cristofolini, T.; Acuña, J.J.S.; Zanetti-Ramos, B.G.; Oliveira, I.R.W.; Soldi, V.; Pasa, A.A.; Creczynski-Pasa, T.B. Characterization of horseradish peroxidase immobilized on PEGylated polyurethane nanoparticles and its application for dopamine detection. *Sens. Actuators B* **2013**, *182*, 264–272. [CrossRef]
37. Zhang, Q.L.; Feng, J.X.; Wang, A.J.; Wei, J.; Lv, Z.Y.; Feng, J.J. A glassy carbon electrode modified with porous gold nanosheets for simultaneous determination of dopamine and acetaminophen. *Microchim. Acta* **2015**, *182*, 589–595. [CrossRef]
38. Wang, J.; Yang, B.B.; Zhong, J.T.; Yan, B.; Zhang, K.; Zhai, C.Y.; Shiraishi, Y.; Du, Y.K.; Yang, P. Dopamine and uric acid electrochemical sensor based on a glassy carbon electrode modified with cubic Pd and reduced graphene oxide nanocomposite. *J. Colloid Interface Sci.* **2017**, *497*, 172–180. [CrossRef] [PubMed]
39. Yang, R.; Zhao, J.; Chen, M.; Yang, T.; Luo, S.; Jiao, K. Electrocatalytic determination of chloramphenicol based on molybdenum disulfide nanosheets and self-doped polyaniline. *Talanta* **2015**, *131*, 619–623. [CrossRef] [PubMed]